Phase behaviour of amphiphilic monolayers: theory and simulation

2001 J. Phys.: Condens. Matter 13 4853

(http://iopscience.iop.org/0953-8984/13/21/313)

INSTITUTE OF PHYSICS PUBLISHING JOURNAL OF PHYSICS: CONDENSED MATTER

J. Phys.: Condens. Matter **13** (2001) 4853–4862 www.iop.org/Journals/cm PII: S0953-8984(01)20072-1

Phase behaviour of amphiphilic monolayers: theory and simulation

D Düchs and F Schmid

Max-Planck-Institut für Polymerforschung, Postfach 3148, 55021 Mainz, Germany
and
Fakultät für Physik, Universität Bielefeld, Universitätsstraße 25, 33615 Bielefeld, Germany

Received 14 December 2000, in final form 5 March 2001

Abstract

Coarse-grained models of monolayers of amphiphiles (Langmuir monolayers) have been studied theoretically and by means of computer simulations. We discuss some of the insights obtained with this approach, and present new simulation results which show that idealized models can successfully reproduce essential aspects of the generic phase behaviour of Langmuir monolayers.

1. Introduction

Amphiphilic molecules are made up of two distinct components: a hydrophilic part which dissolves easily in water ('loves water'), and a hydrophobic part which is repelled by water ('fears water'). In an aqueous environment, they assemble such that the hydrophobic parts of the molecules are shielded from the water by the hydrophilic ones. As a result, a rich variety of ordered and disordered structures emerge, featuring internal 'interfaces' that separate hydrophobic from hydrophilic regions [1].

Among these, bilayer structures are receiving special attention because they are fundamental ingredients of biological membranes and, thus, basic constituents of all living organisms [2]. They are typically formed by molecules which have one hydrophilic 'head group' attached to one or more hydrophobic hydrocarbon chains, e.g., lipids or fatty acids. In water, the molecules may, in certain parameter regions, aggregate into stacks of planar bilayers. These lamellar phases often exist in several variations: with decreasing temperature, they undergo a first-order transition ('main transition') from a high-temperature 'fluid' phase to a low-temperature 'gel' phase, which is characterized by higher bilayer thickness, lower chain mobility, and higher chain ordering. Depending on the chain length and the bulkiness of the polar head group, different gel phases can be found, some with chains oriented on average perpendicular to the lamellar surface, and some with collectively tilted chains. In systems with bulky head groups, the strictly planar gel phase is often pre-empted by one with asymmetric wavy undulations ('ripple' phase). Theoretical considerations have suggested that the latter may be related to tilt order in the bilayers [3]. From an experimental point of view, the question of whether the chains in the ripple phase are tilted or not is still debated [4, 5]. In biological systems, membranes are usually maintained in the fluid state by the living organism.

0953-8984/01/214853+10$30.00

Nevertheless, the main transition is presumably of some relevance in the biological context, as it occurs at temperatures very close to the body temperature for some of the most common bilayer lipids (e.g., 41.5 °C in DPPC).

To assess phenomena of this type, people have been studying Langmuir monolayers for many years as model systems that are particularly accessible in experiments [6]. Such monolayers form when amphiphilic molecules of sufficient chain length are spread onto an air–water interface. At low surface coverage, the molecules do not interact with each other and form what is the two-dimensional analogue of a gas. Upon compression, the system exhibits a first-order 'gas–liquid' transition to a phase where the molecules form a continuous monolayer whose behaviour resembles, in some sense, that of the corresponding bilayer. In particular, one observes a monolayer equivalent of the main transition—a first-order transition between two liquid states: the 'liquid expanded' (LE) and the 'liquid condensed' (LC) state. As in the bilayer case, several phases are present in the condensed region, which differ in the tilt order of the chains, the orientational order of the backbones, and the positional order of the heads. In the phases which coexist with the liquid expanded phase, the molecules are axially symmetric and form a hexatic liquid. A generic phase diagram is shown in figure 1 [7].

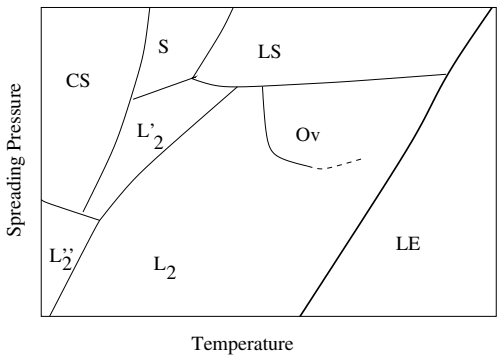

Figure 1. The generic phase diagram for fatty acid monolayers (according to reference [7]). LE is the liquid expanded phase; CS and L_2' have positional order; all other phases are hexatic liquids. The phases Ov and L_2' show tilt towards nearest neighbours, L_2 and L_2' tilt towards next-nearest neighbours, and LS, S, CS are untilted. In CS, S, L_2', and L_2', the backbones of the hydrocarbon chains are ordered.

Interestingly, many topological features of the phase diagram in the condensed region (sequence and order of phase transitions, etc) can be understood in terms of generic Landau symmetry considerations [8]. The impressive results of this approach have been summarized nicely in a recent review article by Kaganer *et al* [9]. Here we will focus our attention on the main transition, i.e., we will consider only the right-hand part of the phase diagram with the liquid expanded phase and the coexisting condensed phases. Our goal is to explore possible explanations of the transitions between those phases using simple idealized models. The paper is organized as follows: first, we will review some theoretical findings, then discuss recent computer simulations and present new results. We hope that we will convince the reader that we are now able to understand and reproduce the relevant characteristics of the experimental phase diagram quite satisfactorily.

2. Theory

Our theoretical work has mainly addressed the following two issues:

(1) What is the mechanism that drives the first-order fluid–fluid transition between the liquid expanded and liquid condensed regions?
(2) Which factors determine tilt order and tilt direction?

The first question was tackled by means of a self-consistent-field theory of a simple grafted chain model [10, 11]. The amphiphiles are modelled as stiff chains of attractive rodlike segments attached to one head segment, which is confined into a planar surface by a harmonic potential and free to move in lateral directions. This model indeed exhibits two coexisting liquid phases, and even an additional tilted phase in certain parameter regions. Two ingredients are crucial in bringing about liquid–liquid coexistence: the flexibility of the chains and an affinity to parallel packing (chain anisotropy). A typical phase diagram is shown in figure 2.

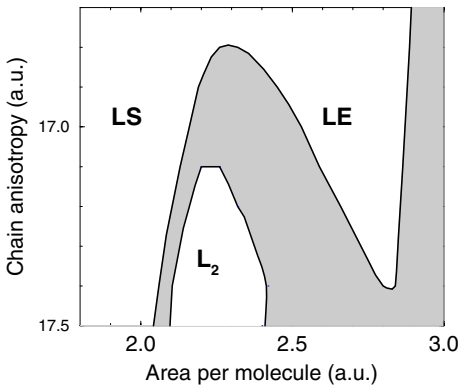

Figure 2. The phase diagram obtained from self-consistent-field calculations in the plane of chain anisotropy versus molecular area. LE denotes liquid expanded phase, LS untilted liquid condensed phase, and L_2 a tilted condensed phase (after reference [9]).

Here, the phase behaviour was plotted as a function of the effective chain anisotropy. An almost identical phase diagram is obtained if the chain anisotropy is kept fixed and the chain stiffness is varied instead. Note that both the effective chain interactions and the effective chain stiffness depend on the temperature. Hence, the y-axis in figure 2 can be interpreted as a temperature axis. Our self-consistent-field calculation does not account for the possibility of hexatic order in the liquid condensed region. This is why the phase coexistence region ends in a critical point, where there should probably be a multicritical point followed, at higher temperatures, by a line of continuous Kosterlitz–Thouless transitions.

Our results show that the liquid–liquid phase transition arises from a competition between the conformational entropy of the chains, which stabilizes the expanded phase, and a tendency to parallel alignment, which stabilizes the condensed phase. The importance of the conformational entropy for the transition had already been demonstrated by experiments of Barton *et al* [12]: if one reduces the chain flexibility by substituting for hydrogen with fluorine, the liquid expanded phase will disappear.

Next, we address the issue of tilt order and tilt direction. The latter is a well-defined quantity in a hexatic liquid since it lacks only positional order and retains long-range bond orientational order [13]. We have studied tilt order in monolayers within an even simpler model than that sketched above, namely a system of rigid rods attached to head groups that are confined into a plane [14]. The main effects are already apparent from an analysis of the state of lowest energy: tilting transitions can be induced by either varying the surface pressure or the head size. In both cases, one finds a sequence of three phases: first an untilted phase (small

heads or high surface pressure), then a phase where the rods are tilted towards next-nearest neighbours, and finally (large heads and low surface pressure) a phase with tilt towards nearest neighbours.

That precise sequence is found experimentally in the pressure–temperature phase diagram (see figure 1). The argument predicts that the phase with tilt towards nearest neighbours should be suppressed if the head groups are too small. This has indeed been observed in experiments, where the effective head size was reduced by increasing the pH of the subphase [15], or by replacing the COOH head groups of fatty acids by smaller alcohol head groups [16, 17].

Note that the theoretical predictions were obtained using a simple model of cylindrical rigid rods. A much more complex ground-state phase behaviour results if in addition the rods are given internal structure. For a model that uses rigid beaded rods, Opps *et al* have found a diversified occurrence of NN to NNN phases depending on the head/tail diameter ratio, bond lengths, and interaction potentials: the head diameters govern the overall tilting behaviour, whereas the finer details of the phase diagram depend on the precise nature of the interaction potentials [18].

To summarize this section, our theoretical studies have shown that much of the phase behaviour in Langmuir monolayers can be discussed in terms of a few elementary properties of amphiphiles: the flexible chains with their tendency to parallel packing drive the transition from liquid expanded to liquid condensed, and the tilting transitions are driven by an interplay between head size, chain diameter, and surface pressure.

In the next section, we will discuss computer simulations of a model which incorporates just these few basic ingredients.

3. Computer simulations

A vast amount of activity has been devoted to the simulation of surfactant systems in general, and bilayers or monolayers in particular. For a general account, we refer the interested reader to recent reviews [19–21] and will only report on our own work here [22–24].

We model the amphiphiles as chains of N beads with diameter σ_T, attached to one slightly larger head bead with diameter σ_H, which is confined to the plane $z = 0$. Beads are not allowed into the half-space $z < 0$. Two beads that are not direct neighbours in the same chain interact with truncated and shifted Lennard-Jones potentials:

$$V_{LJ}(r) = \begin{cases} \epsilon((\sigma/r)^{12} - 2(\sigma/r)^6 + v_c) & \text{for } r \leqslant R_0 \\ 0 & \text{for } r > R_0 \end{cases} \tag{1}$$

where the offset v_c is chosen such that $V_{LJ}(r)$ is continuous at $r = R_0$, and the cut-off R_0 is $R_0 = 2\,\sigma_T$ for the tail beads and $R_0 = \sigma_H$ for the head beads. Hence, tail beads attract each other and head beads are purely repulsive. The interactions between head and tail beads are repulsive with the effective diameter $(\sigma_T + \sigma_H)/2$. Beads are connected by springs of length d subject to the weakly nonlinear spring potential

$$V_S(d) = \begin{cases} -\dfrac{k_S}{2} d_S^2 \ln[1 - (d - d_0)^2/{d_S}^2] & \text{for } |d - d_0| < d_S \\ \infty & \text{for } |d - d_0| > d_S. \end{cases} \tag{2}$$

Moreover, a stiffness potential

$$V_A = k_A(1 - \cos\theta) \tag{3}$$

is imposed, which acts on the angle θ between subsequent springs and favours $\theta = 0$ (straight chains). Unless stated otherwise, the model parameters are $d_0 = 0.7\,\sigma_T$ (equilibrium spring

length), $d_S = 0.2\ \sigma_T$, $k_S = 100\epsilon$, $k_A = 10\epsilon$, and $\sigma_H = 1.1\ \sigma_T$. In most cases, systems of 144 chains with a total length of 7 beads were studied. A preliminary discussion of chain end and system size effects can be found in reference [23]. The simulations were conducted at constant spreading pressure Π in a simulation box of variable size and shape, with periodic boundary conditions in the x- and y-directions.

Quantities of special interest are the collective tilt of the chains and the liquid structure. The collective tilt is measured with the order parameter

$$R_{xy} = \sqrt{\langle [x]^2 + [y]^2 \rangle} \tag{4}$$

where $[x]$ and $[y]$ denote the x- and y-components, respectively, of the head-to-end vector of a chain, averaged over all chains in one configuration, and $\langle \cdot \rangle$, the statistical average over all configurations. To study the liquid structure, we have inspected radial pair correlation functions and the hexagonal order parameter of two-dimensional melting:

$$\Psi_6 = \left\langle \left| \frac{1}{6n} \sum_{j=1}^{n} \sum_{k=1}^{6} \exp(\mathrm{i}\, 6\phi_{jk}) \right|^2 \right\rangle \tag{5}$$

which measures the orientational long-range order of nearest-neighbour directions. Here the sum j runs over all heads of the system, the sum k, over the six nearest neighbours of j, and Φ_{jk} is the angle between the vector connecting the two heads and an arbitrary reference axis.

At head size $\sigma_H = 1.1\ \sigma_T$, we find four different phases: a disordered liquid (LE) and three condensed phases, one without tilt (LC-U), one with tilt towards nearest neighbours (LC-NN), and one with tilt towards next-nearest neighbours (LC-NNN). Our systems are too small to allow for dislocations, and the molecules are almost always arranged on a defect-free lattice in the condensed region. However, hexatic disorder may well be present in larger systems. The phase diagram in the pressure–area plane, obtained by inspection of the order parameters R_{xy} and Ψ_6, as well as by a phonon expansion at low temperatures [22], is plotted in figure 3.

We are now in a position to compare the simulations with some of the theoretical results. Figure 4 shows examples of radial pair correlation functions for head beads and whole chains at temperatures well below, slightly below, slightly above, and well above the LE/LC transition temperature. One notices that the correlation function of whole chains changes quite dramatically at the phase transition, whereas the head correlation function remains rather unaffected. The chains maintain the order below the transition, and promote disorder above the transition. In agreement with the theoretical prediction, one can conclude that the chains drive the transition.

At low temperatures, the model exhibits the sequence of tilting transitions predicted by the theory (see figure 3), with a first-order transition between the two tilted phases. At higher temperatures, the situation is less clear. The direct inspection of several configuration snapshots suggests that the system might pass directly from the LC-NN phase to the LC-U phase, skipping the intermediate LC-NNN state. Unfortunately, the tilt direction fluctuates so strongly that the average direction cannot be determined unambiguously. Simulations of much larger systems would be needed to clarify this aspect of the phase diagram.

If one increases the head size, the region where the chains tilt towards nearest neighbours becomes larger, as anticipated by the theory. Interestingly, this goes along with the appearance of a new, unexpected LC-NN modification: a modulated striped phase [23]. It proves to be extremely stable over a wide parameter region. One may speculate on their existence in real systems.

Although the phase diagram of figure 3 is already gratifyingly similar to the experimental phase diagram (figure 1), it still contains one obvious flaw: the pressure at the transition between tilted and untilted phases is largely temperature independent in experiments, whereas it has

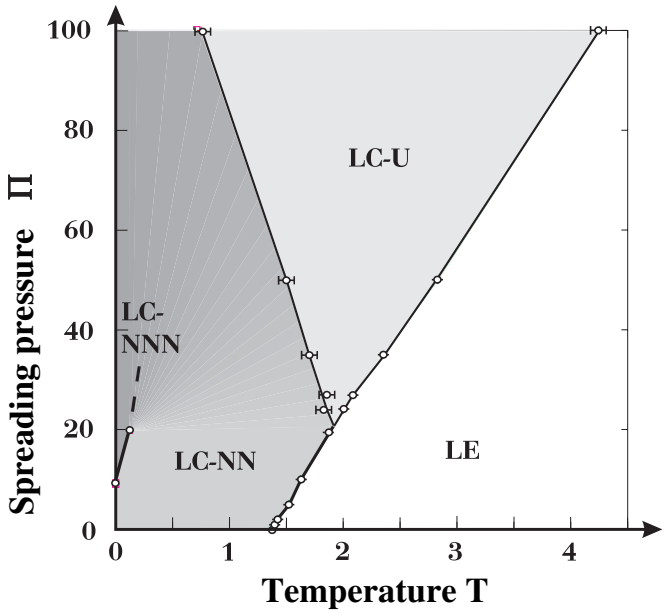

Figure 3. The phase diagram obtained from Monte Carlo simulations in the plane of spreading pressure Π (in units of $\epsilon/k_B\sigma_T^2$) versus temperature T (in units of ϵ/k_B). LE denotes disordered phase, LC-U untilted ordered phase, LC-NN ordered phase with tilt towards nearest neighbours, and LC-NNN ordered phase with tilt towards next-nearest neighbours. At pressures above $\Pi = 20\epsilon/\sigma_T^2$, the tilt direction is unclear. (After reference [20].)

a considerable slope in the simulations. The most plausible explanation for this discrepancy is to attribute it to the overly simple treatment of the head groups, or, more precisely, to the rigid constraints imposed on them. The slope of the phase boundary can easily be rationalized if one assumes that the heads are forced to absorb most of the pressure because they cannot move out of their plane.

In order to remedy this situation, we have conducted a set of simulations where the surface constraints are softened up and replaced by harmonic surface potentials [24]. The main results of this study will be presented now.

The new surface potentials were chosen as follows. Head beads are subject to a potential

$$V_h(r) = \begin{cases} 0 & \text{for } z < -0.5W \\ -(\epsilon_h/2)\ln(1-(z+0.5W)^2/W^2) & \text{for } -0.5W < z < 0.5W \end{cases} \tag{6}$$

and tail beads to a potential

$$V_t(r) = \begin{cases} (-\epsilon_t/2)\ln(1-(z-0.5W)^2/W^2) & \text{for } -0.5W < z < 0.5W \\ 0 & \text{for } z > 0.5W. \end{cases} \tag{7}$$

The width W of the potential is set to 1 σ_T, and the strength factors ϵ_h and ϵ_t are given the values 10ϵ. As we will see, the exact form of the surface potentials is not crucial.

Apart from this innovation, the model is defined as before, with the one exception that the stiffness potential was reduced to $k_A = 4.7\epsilon$. This is the value which one would estimate from the Rigby–Roe model for hydrocarbon chains [25], assuming that two carbon atoms correspond roughly to one bead in our model. The size of the head bead was chosen as $\sigma_H = 1.1\ \sigma_T$, as in the study discussed above.

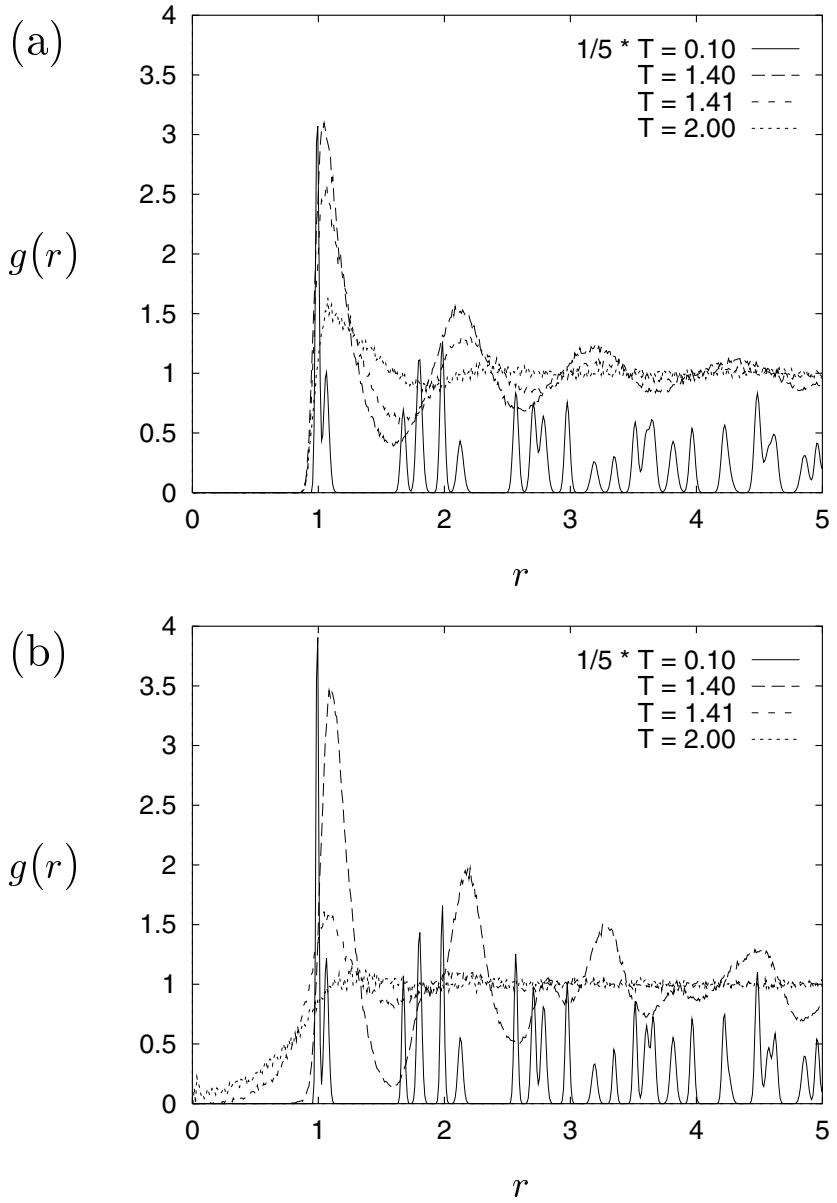

Figure 4. The radial pair correlation function $g(r)$ for the heads (a) and the projections of the centres of gravity into the xy-plane (b) versus r (in units σ_T) at spreading pressure $\Pi = 1\ \epsilon/\sigma_T^2$ and various temperatures (in units ϵ/k_B), as indicated. The phase transition from LE to LC-NN takes place at temperature $T = 1.4\epsilon/k_B$. The values $g(r)$ for the temperature $T = 0.1\epsilon/k_B$ are rescaled by a factor of 5. (After reference [20].)

The results can be summarized as follows.

We find essentially the same phases and the same phase characteristics as before. As an unwanted artefact of the model, one observes at low temperatures and high pressures a double-peak structure in the head density profile $\rho_h(z)$. Fortunately, the effect disappears at temperatures $T > 0.5\epsilon/k_B$, and the system is well behaved in all parameter ranges of interest.

As we had hoped, the transition pressures of the tilting transition at lower temperatures drop considerably. In order to explore the sensitivity of the phase behaviour to the parameters of the new surface potentials, we have performed a few simulation runs of systems with double potential width W. Results for an exemplary isotherm are shown in figure 5: the phase transition occurs at almost the same pressure in systems with potential width $W = \sigma_T$ and $W = 2\,\sigma_T$. The transition pressure is much lower than that in the original model (cf. figure 3). Hence, a dramatic lowering of the transition pressures is achieved by a mere relaxation of the head groups. Once this lowering is accomplished, further relaxation does not have much impact.

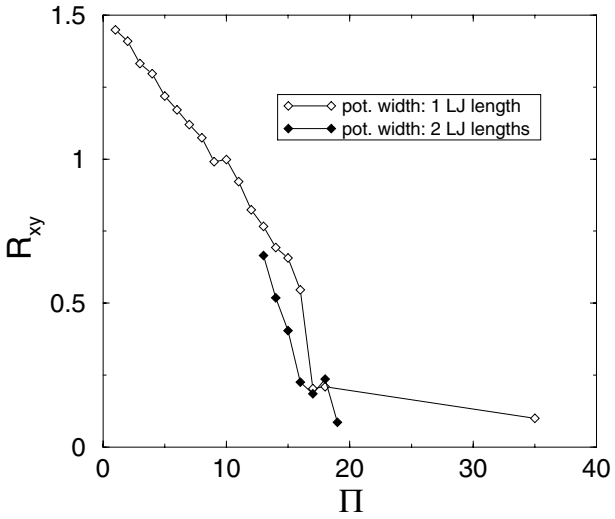

Figure 5. Collective tilt order parameter R_{xy} versus pressure Π in units $\epsilon/k_B\sigma_T^2$ at temperature $T = 0.5\epsilon/k_B$ for different potential widths (units $\epsilon/k_B\sigma_T$) versus temperature T (units ϵ/k_B).

Another new feature of the model, compared with the earlier version, concerns the order of the tilting transition. Whereas in the old version, we had no reason to doubt that it is continuous (although this really ought to be established rigorously by a finite-size analysis, of course), the order parameter R_{xy} now seems to jump between two states in the vicinity of the transition. A typical histogram of R_{xy} is shown in figure 6. One clearly discerns two peaks, corresponding to two states of different tilt order. This observation suggests that the tilting transition might be first order. Again, simulations of much larger systems would be needed to corroborate this suspicion.

The phase diagram of the revised model is shown in figure 7. The changes to the LE/LC boundary compared to the earlier version (figure 3) are rather marginal; it experiences only a small shift to lower temperatures. However, the boundary between the tilted and untilted phases is affected in the desired dramatic way: the transition pressures at lower temperatures drop considerably, and the slope of the transition line is now almost flat, like in experiments.

We conclude that we have established a minimal model which reproduces in computer simulations the essential features of the experimentally observed generic phase behaviour of Langmuir monolayers. Details of the phase diagram will still need to be established by systematic finite-size studies. We note that long-range Coulomb and dipolar interactions have not been included in the model so far. In the coexistence region of the liquid expanded and liquid condensed states, the interplay between electrostatic interactions and line tensions leads

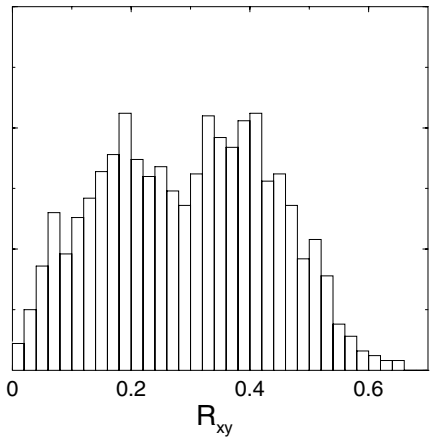

Figure 6. Distribution of the order parameter R_{xy} at spreading pressure $\Pi = 15\epsilon/k_B\sigma_T^2$ and temperature $T = 1.3\epsilon/k_B$.

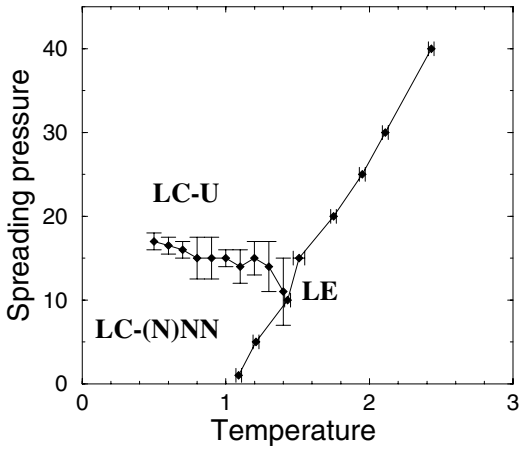

Figure 7. The phase diagram from Monte Carlo simulations of the model with soft surface potentials in the plane of spreading pressure Π (units $\epsilon/k_B\sigma_T^2$) versus temperature T (units ϵ/k_B). LE denotes disordered phase, LC-U untilted ordered phase, and LC-NN(N) ordered phase with tilt towards nearest or next-nearest neighbours (undetermined).

to a variety of interesting domain patterns on a mesoscopic scale [6]. On the microscopic scale considered here, however, these long-range interactions seem less influential. We feel that the general agreement between the phase behaviour of the model and the experimental one is now satisfactory enough for us to use the model as a basis for the investigation of more complex problems.

Acknowledgments

Part of the work presented here was done in collaboration with M Schick, C Stadler, and H Lange. We thank N Akino, K Binder, F M Haas, R Hilfer, and S Opps for enjoyable interactions and useful discussions.

References

[1] Gompper G and Schick M 1994 *Self-Assembling Amphiphilic Systems (Phase Transitions and Critical Phenomena vol 16)* ed C Domb and J L Lebowitz (London: Academic)
[2] Gennis R B 1989 *Biomembranes* (Berlin: Springer)
[3] Lubensky T C and Mackintosh F C 1993 *Phys. Rev. Lett.* **71** 1565
[4] Sengupta K, Rahunathan V A and Katsaras J 2000 *Europhys. Lett.* **49** 722
[5] Nagle J F and Tristam-Nagle S 2000 *Curr. Opin. Struct. Biol.* **10** 474
[6] Möhwald H 1990 *Annu. Rev. Phys. Chem.* **41** 441
McConnell H M 1991 *Annu. Rev. Phys. Chem.* **42** 171
Knobler C M and Desai R C 1992 *Annu. Rev. Phys. Chem.* **43** 207
[7] Bibo A M and Peterson I R 1990 *Adv. Mater.* **2** 309
Peterson I R, Brzezinski V, Kenn R M and Steitz R 1992 *Langmuir* **8** 1992
Overbeck G A and Möbius D 1993 *J. Phys. Chem.* **97** 7999
Rivière S, Hénon S, Meunier J, Schwartz D K, Tsao M-W and Knobler C M 1994 *J. Chem. Phys.* **101** 10 045
[8] Kaganer V M, Opisov M A and Peterson I R 1992 *J. Chem. Phys.* **98** 3512
Kaganer V M and Indenbom V L 1993 *J. Physique* II **3** 813
Kaganer V M and Loginov E B 1993 *Phys. Rev. Lett.* **71** 2599
Kaganer V M and Loginov E B 1995 *Phys. Rev.* E **51** 2237
[9] Kaganer V M, Möhwald H and Dutta P 1999 *Rev. Mod. Phys.* **71** 779
[10] Schmid F and Schick M 1995 *J. Chem. Phys.* **102** 2080
[11] Schmid F 1997 *Phys. Rev.* E **55** 5774
[12] Barton S W, Thomas B N, Flom E B, Rice S A, Lin B, Peng J B, Ketterson J B and Dutta P 1988 *J. Chem. Phys.* **89** 2257
[13] Halperin B I and Nelson D R 1978 *Phys. Rev. Lett.* **41** 121
[14] Schmid F and Lange H 1997 *J. Chem. Phys.* **106** 3757
[15] Shih M C, Bohanon T M, Mikrut J M, Zschack P and Dutta P 1992 *J. Chem. Phys.* **96** 1556
[16] Fischer B, Teer E and Knobler C M 1995 *J. Chem. Phys.* **102** 2365
[17] Teer E, Knobler C M, Lautz C, Wurlitzer S, Kildae J and Fischer T M 1997 *J. Chem. Phys.* **106** 1913
[18] Opps S B, Nickel B G, Gray C G and Sullivan D E 2000 *J. Chem. Phys.* **113** 339
[19] Liverpool T B 1996 *Annual Review of Computational Physics* vol 4, ed D Stauffer (Singapore: World Scientific) p 317
[20] Schmid F 2000 *Computational Methods in Surface and Colloid Science (Surfactant Science Series vol 89)* ed M Borowko (New York: Dekker) p 631
[21] Shelley J C and Shelley M Y 2000 *Curr. Opin. Colloid Interface Sci.* **5** 101
Bandyopadhyay S, Tarek M and Klein M L 1998 *Curr. Opin. Colloid Interface Sci.* **3** 242
Larson R G 1997 *Curr. Opin. Colloid Interface Sci.* **2** 361
Tobias D J, Tu K and Klein M L 1997 *Curr. Opin. Colloid Interface Sci.* **2** 15
Karaborni S and Smit B 1996 *Curr. Opin. Colloid Interface Sci.* **1** 411
[22] Stadler C, Lange H and Schmid F 1999 *Phys. Rev.* E **59** 4248
[23] Stadler C and Schmid F 1999 *J. Chem. Phys.* **110** 9697
[24] Düchs D 1999 *Diploma Thesis* Universität Mainz, Germany
[25] Rigby D J and Roe R J 1987 *J. Chem. Phys.* **87** 7285